Available online at www.sciencedirect.com
ScienceDirect
Applied Surface Science 254 (2007) 303–307
applied surface science
www.elsevier.com/locate/apsusc

Low-cost 3D nanocomposite solar cells obtained by electrodeposition of $CuInSe_2$

M. Valdés [a,b], M.A. Frontini [a], M. Vázquez [a,*], A. Goossens [b]

[a] *División Corrosión, INTEMA, Facultad de Ingeniería, Universidad Nacional de Mar del Plata, J.B. Justo 4302, B7608FDQ Mar del Plata, Argentina*
[b] *Optoelectronic Materials, Faculty of Applied Sciences, Delft University of Technology, Julianalaan 136, 2628 BL Delft, The Netherlands*

Available online 10 July 2007

Abstract

Thin $CuInSe_2$ films have been prepared by electrodeposition from a single bath aqueous solution on both dense and nanoporous TiO_2. The films are deposited potentiostatically using a N_2-purged electrolyte at different potentials. Various deposition times and solution compositions have been employed. The effect of annealing in air and in argon at different temperatures and times is also investigated. Thin films and nanocomposites of TiO_2 and $CuInSe_2$ have been studied with electron microscopy, X-ray diffraction, Raman spectroscopy, and optical absorption spectroscopy. After a thermal anneal in argon at 350 °C for 30 min excellent $CuInSe_2$ is obtained. In particular the nominal crystal structure and the bandgap of 1.0 eV are found. Although pinholes are present occasionally, good samples with diode curves showing a rectification ratio of 24 at ±1 V are obtained. Upon irradiation with simulated solar light of 1000 W m^{-2} a clear photoconductivity response is observed. Furthermore, also some photovoltaic energy conversion is found in $TiO_2|CuInSe_2$ nanocomposites.

PACS : 73.40.Kp; 73.50.Pz

Keywords: TiO_2; Nanoporous; CISe; Electrodeposition; Solar cells

1. Introduction

In order to reduce the production cost of solar cells, new cell concepts based on nanostructured materials have been developed. Grätzel and co-workers introduced an important advancement by using nanostructured titanium dioxide in dye-sensitized solar cells [1]. Others authors have used a similar concept to design new cells based on 3D inorganic hetero-junctions, achieving conversion efficiencies of 5% using atomic layer deposition (ALD) and spray pyrolysis deposition (SPD) [2,3].

It is recognized that significant reduction of the production costs can be achieved if solar cells can be obtained under mild conditions and preferably without vacuum. Electrodeposition of chalcogenides has emerged as an alternative low-cost method for thin film solar cell production reaching remarkable conversion efficiencies [4–7]. Most authors have used metals or metallic coated glasses as substrate for electrodeposition.

In the present study, an inorganic heterojunction based in nanocomposite of TiO_2 (n-type semiconductor) and $CuInSe_2$ (p-type semiconductor) is pursued using electrodeposition. In a nanocomposite of TiO_2 and $CuInSe_2$ the pn junction is distributed in space, which allows reduction of the minority carrier diffusion length down to a few tens of nanometers. Exploring the variables associated to the electrodeposition process and thermal annealing to maximise the energy conversion efficiency of solar cells is the focal point of our current investigations.

2. Experimental

Glass coated with a transparent conducting oxide (TCO, Libbey Owens Ford, TEC 8/3 mm) is used as the substrate and is degreased in an ultrasonic bath with ethanol three times during 15 min.

Spray deposition is then applied to deposit a dense 150 nm thin film of anatase TiO_2 [8]. This film prevents direct contact

* Corresponding author at: División Corrosión, INTEMA, Facultad de Ingeniería, UNMdP, Juan B. Justo 4302, B7608FDQ Mar del Plata, Argentina. Tel.: +54 223 481 6600; fax: +54 223 481 0046.
E-mail address: mvazquez@fi.mdp.edu.ar (M. Vázquez).

0169-4332/$ – see front matter © 2007 Elsevier B.V. All rights reserved.
doi:10.1016/j.apsusc.2007.07.063

between $CuInSe_2$ and SnO_2:F (TCO), which short-circuits the cell. Next, a nanocrystalline anatase TiO_2 (nc-TiO_2) coating is applied using doctor blading [9]. These films consist of 9 nm or 25 nm crystallites sintered together at 450 °C for 6 h to form the electron-conducting matrix with a thickness of approximately 1 μm.

Electrodeposition of $CuInSe_2$ (CISe) is carried out at room temperature using aqueous solutions with different Cu:In:Se ratios in the electrolyte (1:1:1, 1:2:1, 1:2:2, 1:4:2). The composition of the aqueous solution used is 5 mM $CuCl_2$, 10 mM $InCl_3$ and 5 mM SeO_2 for the 1:2:1 electrolyte ratio and similar for the others. The pH of the bath is adjusted between 1.5 and 2.5 using diluted HCl solution. During the electrodeposition the solution is purged with nitrogen and bath temperature is maintained at room temperature. CISe thin films are deposited potentiostatically, using a three electrodes configuration. A standard calomel electrode (SCE) is used as reference and a Pt sheet of big area is the counter electrode. The substrates are square (2 cm × 2 cm) TiO_2 coated TCO glasses, as previously described. The electroactive geometrical area is confined by the cell design to 1.13 cm^2, but one should take into account that the internal surface area of nc-TiO_2 is much larger.

The electrodeposition process is controlled using a Princeton Applied Research Potentiostat/Galvanostat model 273. The films have been deposited at 4 different potentials varying between −0.7 and −1.0 V versus SCE during 60 min.

To improve the crystallinity of the as-deposited CISe films a post-deposition annealing is carried out at different temperatures between 300 and 450 °C in argon atmosphere.

The excess of Cu and Se is removed by etching the films in 0.5 M KCN aqueous solution for different periods of time (1–5 min) as is described in the literature [10].

The crystal structure of the samples is determined with X-ray diffraction (Bruker D8 Advanced Diffractometer) using Cu K_α radiation and Ni–Cu slits filter. The operation voltage and current used are 40 kV and 40 mA, respectively. The diffraction patterns are recorded from $2\theta = 10^\circ$ to 70°. Raman spectra are obtained using a Spectra Physics Millenia Nd:YVO_4 with a wavelength of 532 nm in the backscattering mode, a set of notch filters to remove the Raleigh scatterings and a 340 Spex monochromator equipped with an 1800 grooves/mm grating.

The optical properties of the films, i.e. absorption coefficient and the direct band gap energy E_g are derived from the transmission spectra.

To investigate the photoresponse of the cells, current–voltage curves of representative devices such as SnO_2:F/TiO_2(100 nm)/CISe/graphite and SnO_2:F/TiO_2(100 nm)/nc-TiO_2/CISe/graphite are performed in the dark and under 1000 W m^{-2} simulated solar irradiation (AM 1.5, K.H. Steuernagel Lichttechnik GmbH). In some samples evaporated gold dots (0.0314 cm^2) are used as back contacts.

3. Results and discussion

3.1. TiO_2 characterization

Fig. 1 presents XRD patterns of dense and nanostructured anatase TiO_2 thin films prepared by spray pyrolysis and doctor blade, respectively. In addition to the peaks related to the substrate (SnO_2:F), the main peaks of anatase TiO_2 (1 0 1) and (2 0 0) at 29.49° and 56.5°, respectively, are found in the diffractogram, indicating good crystallinity of the material. In the case of nc-TiO_2 of 25 nm an small peak of rutile at 32° is also present. Fig. 2 presents a Raman spectrum of nc-TiO_2. The particle size in this case is 25 nm (Degussa, P25). Intense Raman scattering saturates the detector.

3.2. CISe characterization

Fig. 3 shows the X-ray diffraction patterns of the CISe film deposited on dense TiO_2 films before and after annealing in argon at 350 °C for 30 min. Annealing significantly improves the crystallinity of the CISe films. In both patterns, the characteristic peaks of the chalcogenite structure (1 1 2), (2 0 4) and (2 0 0/1 1 6) are present but only after annealing the peaks become narrow and intense, indicating full crystallization of the $CuInSe_2$ with a preferred orientation in the

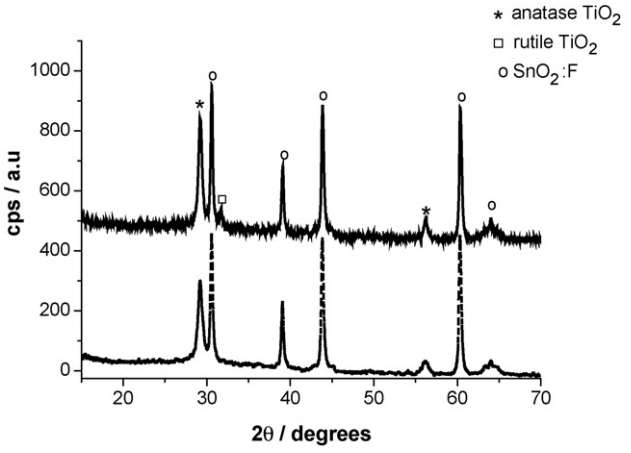

Fig. 1. XRD patterns of TCO/dense TiO_2/nc–TiO_2. nc-TiO_2 average particle size is 25 nm (full line) and 9 nm (dash line).

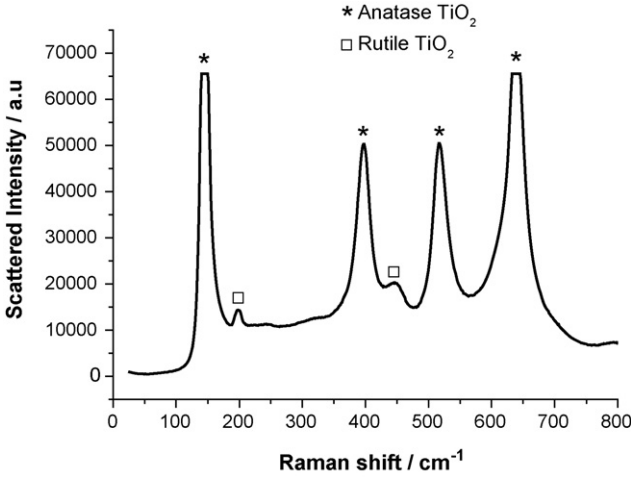

Fig. 2. Raman spectrum of nc-TiO_2 (25 nm) deposited by doctor blade on TCO substrate.

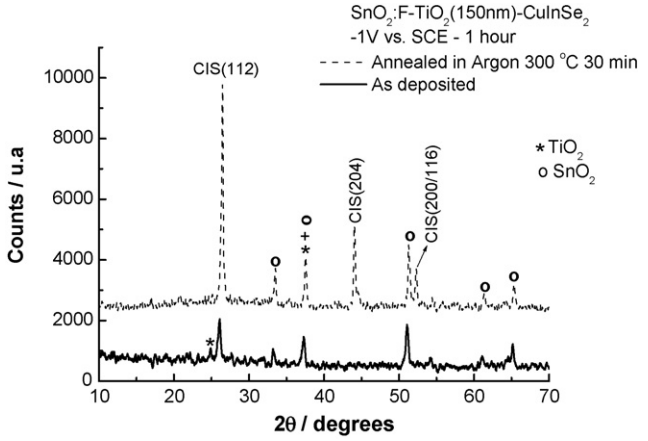

Fig. 3. XRD patterns of CISe films at −1 V vs. SCE after 1 h of deposition showing the annealing effect on the crystallinity of CISe.

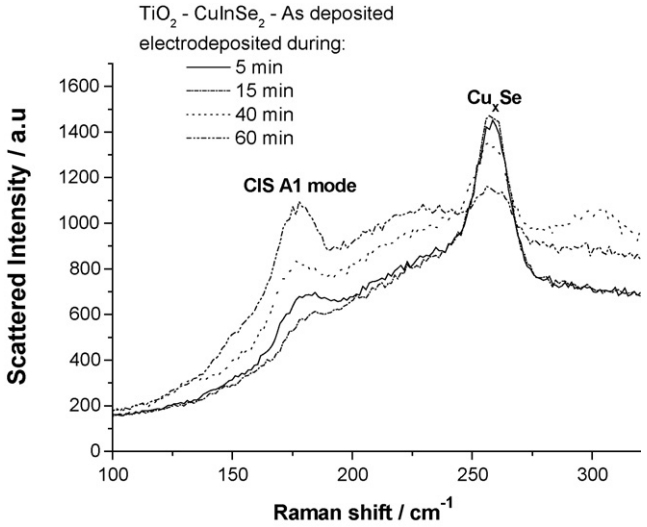

Fig. 5. Raman spectra of as-deposited CISe films at different deposition times.

(1 1 2) orientation. The others peaks are attributed to the TiO_2 and SnO_2 layers.

Absorption spectra are recorded for as-deposited and annealed samples prepared at various potentials and deposition times. These data can be converted into $(\alpha h\nu)^2$ versus $(h\nu)$ plots, so as to determine the band gap values (E_g) of the films. The calculated E_g values of as-deposited CISe or for samples annealed under various conditions vary between 0.9 and 1.0 eV and are shown in Fig. 4. E_g values of films produced at different potentials or for different deposition times were found to be always close to 1.0 eV, in agreement with the reported values for the electrodeposited CISe thin films [11].

Typical Raman spectra of as deposited CISe films on dense TiO_2 at different deposition times are presented in Fig. 5. The intensity of Raman peaks strongly depends on the surface morphology and the phase composition of the CISe films.

All the spectra contain the A1 mode between 175 and 178 cm^{-1}, generally observed in $CuInSe_2$, and an additional peak at 258 cm^{-1} [12]. The latter peak is related to the presence of a Cu_xSe secondary phase. At short deposition times (5 and 15 min) Cu_xSe seems to be dominant with respect to the CISe phase in the film but at longer deposition times (45 and mainly 60 min) the fraction of Cu_xSe phase becomes smaller. From this observation we postulate that the electrodeposition of CISe is induced by an initial deposition of $CuSe_x$ which later transforms into $CuInSe_2$.

A well-known method to remove the Cu_xSe phase is etching the film in KCN. Etching can be done before or after the annealing the CISe films. When as-deposited films are etched in KCN, partial detachment of the film occurs already after 1 min. On the other hand, when annealed CISe films are etched, detachment no longer occurs. Therefore, in this work, all etching experiments are performed on annealed CISe films.

Fig. 6 shows Raman spectra of an annealed CISe film before and after a KCN etch. The signal at 258 cm^{-1}, related to a Cu_xSe phase, is almost completely eliminated by etching.

Fig. 7 shows a SEM micrograph of a CISe film deposited on dense TiO_2/nc-TiO_2. CISe films annealed at 350 °C show bigger particles, in the micrometer range, as preferred in solar cells.

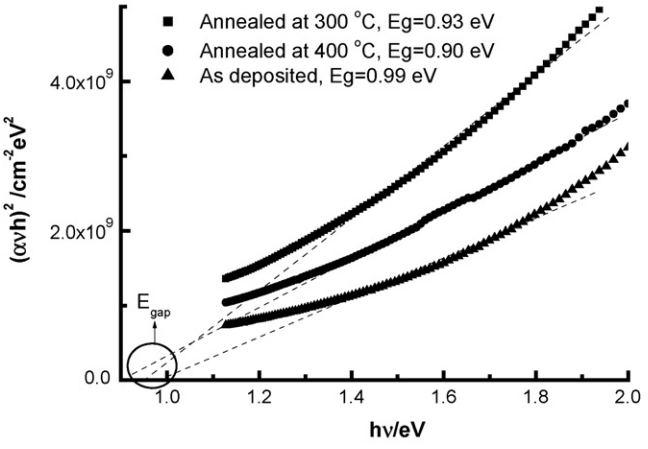

Fig. 4. Plots of $(\alpha h\nu)2$ vs. $(h\nu)$ for CISe films. The films have been deposited at −0.9 V during 1 h. (▲) as-deposited, $E_g = 0.99$ eV; (■) annealed in Ar at 300 °C during 30 min, $E_g = 0.93$ eV; (●) annealed in Ar at 400 °C during 30 min, $E_g = 0.90$ eV.

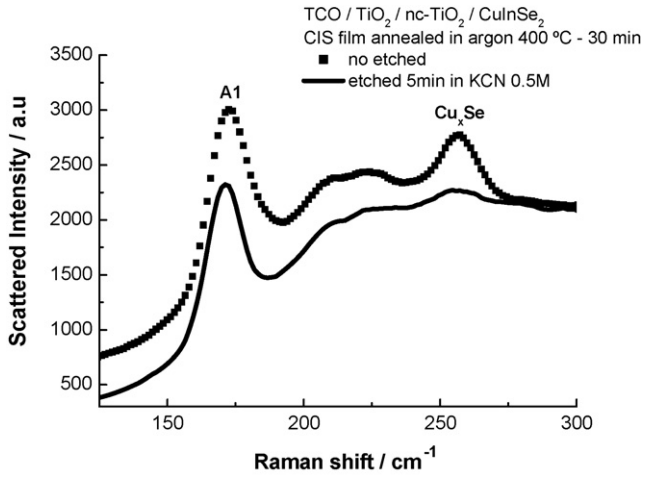

Fig. 6. Raman spectra of annealed CISe films, before and after etching in KCN.

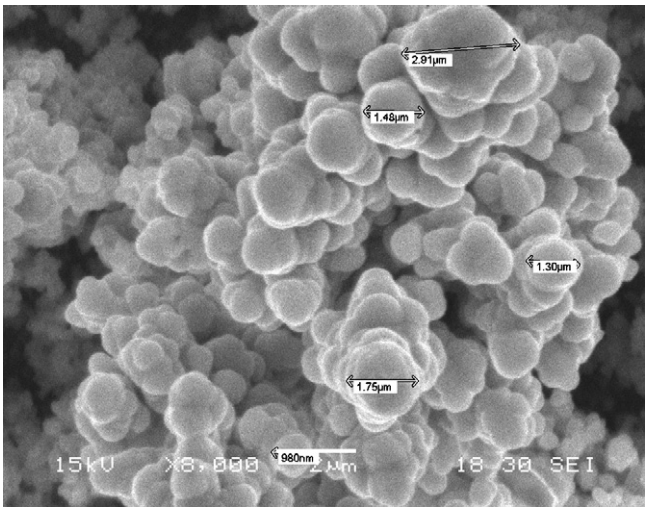

Fig. 7. SEM micrograph of CISe film on TiO_2 annealed at 350 °C in argon during 30 min.

3.3. I–V characterization

Fig. 8 presents the dark *I–V* response of the TiO_2—gold Schottky barrier. This is a simple measurement that can be used to check if the quality of the dense and nanocrystalline TiO_2 is good enough to be used in a solar cell device. The low current density values can be related with the resistance and thickness of the TiO_2/nc–TiO_2 (bi)layer. Despite this, the *I–V* curve behaves like that of a diode, with a resulting rectification ratio of 24 at +1 and −1 V.

The first solar cell device obtained at the moment is shown in Fig. 9. It consisted of SnO_2:F/TiO_2(100 nm)/nc-TiO_2/CISe/graphite. nc-TiO_2 has been prepared using 9 nm particles and the CISe is electrodeposited from a single bath, at −0.8 V for 1 h. Annealed at 350 °C in Ar during 30 min is performed. No further etching is carried out. Despite the low values of the open circuit potential (V_{oc}) and the short-circuit current density (J_{sc}) this is an interesting result since it implies that it is possible to electrodeposit CISe inside the pores of nc-TiO_2. By optimizing the annealing and etching processes, the conversion efficiency is expected to improve significantly.

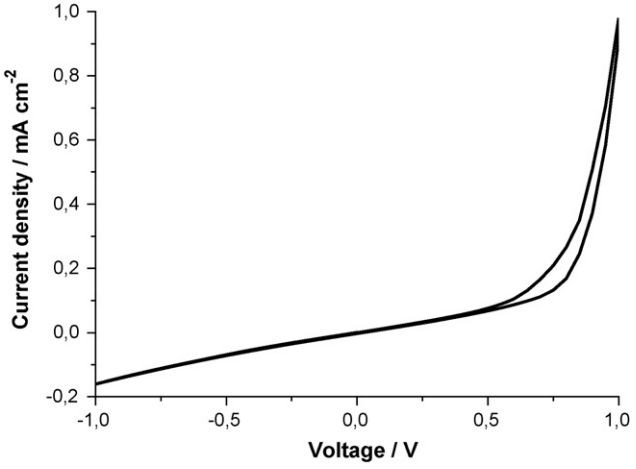

Fig. 8. Dark *I–V* response of SnO_2:F/dense TiO_2/nc-TiO_2 (9 nm)/gold dot cell configuration.

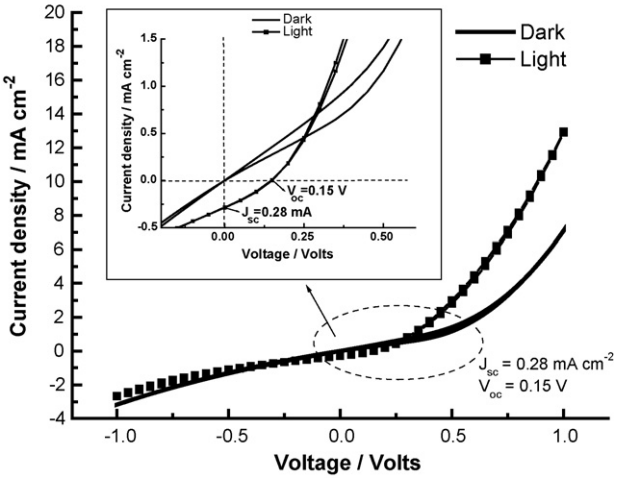

Fig. 9. *I–V* curves recorded in the dark and under illumination of a cell consisting of SnO_2:F/TiO_2(100 nm)/nc-TiO_2/CISe/graphite. CISe is electrodeposited at −0.8 V during 1 h and annealed at 350 °C in Ar during 30 min.

Fig. 9 shows a photoconductivity of a factor 2 at 1 V, while the photocurrent is 0.28 mA cm^{-2}. Fast electron–hole recombination destroys most of the photovoltaic activity. By applying a buffer layer we expect to accomplish significant reduction of the back reaction and hence an improvement of the energy conversion efficiency.

4. Conclusions

Anatase TiO_2 with a good semiconductor quality can be obtained by chemical spray pyrolysis deposition and doctor blading of nanoparticles, respectively. The integrity of the dense anatase TiO_2 film is very important to avoid pinholes. The thickness and resistance of this dense TiO_2 film is restricted to allow uniform and homogenous electrodeposition of $CuInSe_2$. A thickness of 150 nm of dense TiO_2 seems to be appropriate to obtain a good electrodeposited CISe film.

$CuInSe_2$ (CISe) has been obtained using one-step electrodeposition showing absorption, XRD and Raman spectra in good agreement with those reported for the crystalline material. When CISe is electrodeposited on top of a duplex layer composed of dense and nanocrystalline TiO_2 a heterojunction is formed.

Here we report the first 3D TiO_2/$CuInSe_2$ nanocomposite solar cell obtained by one-step electrodeposition of CISe. The low energy conversion in the illuminated *I–V* curve can be related with fast electron–hole recombination in the TiO_2/CISe interface. Current studies focus on introducing a buffer layer and on rapid thermal annealing in sulfur.

References

[1] B. O'Regan, M. Grätzel, Nature 353 (1991) 737.
[2] M. Nanu, J. Schoonman, A. Goossens, Adv. Mater 16 (2004) 453.
[3] M. Nanu, J. Schoonman, A. Goossens, Nanoletters 5 (2005) 1716.
[4] R.N. Bhattacharya, H. Wiesner, J. Electrochem. Soc. 145 (1998) 3435.

[5] J. Barker, S.P. Binns, D.R. Johnson, et al. Int. J. Solar Energy 12 (1992) 79.
[6] A. Kampmann, R. ReinekeKoch, Prog. Photovolt. Res. Appl. 7 (1999) 129.
[7] D. Lincot, J.F. Guillemoles, S. Taunier, Solar Energy 77 (2004) 725.
[8] L. Kavan, M. Grätzel, Electrochim. Acta 40 (1995) 643.
[9] M.K. Nazeeruddin, A. Kay, I. Rodicio, R. Humphry-Baker, E. Muller, P. Liska, N. Vlachopoulos, M. Grätzel, J. Am. Chem. Soc. 115 (1993) 6382.
[10] M. Kemell, M. Ritala, M. Leskela, J. Mater. Chem. 11 (2001) 668.
[11] N. Stratieva, I. Tomov, Sol. Energy Mater. Sol. Cells 45 (1997) 87.
[12] J.H. Park, I.S. Yang, H.Y. Cho, Appl. Phys. A 58 (1994) 125.